Korean J. Chem. Eng., **30**(3), 693-699 (2013)
DOI: 10.1007/s11814-012-0198-6

Structural properties of water around uncharged and charged carbon nanotubes

Amir Reza Ansari Dezfoli*, Mozaffar Ali Mehrabian*,†, and Hassan Hashemipour Rafsanjani**

*Department of Mechanical Engineering, Shahid Bahonar University of Kerman, Iran
**Department of Chemical Engineering, Shahid Bahonar University of Kerman, Iran
(*Received 23 April 2012 • accepted 11 November 2012*)

Abstract−Studying the structural properties of water molecules around the carbon nanotubes is very important in a wide variety of carbon nanotubes applications. We studied the number of hydrogen bonds, oxygen and hydrogen density distributions, and water orientation around carbon nanotubes. The water density distribution for all carbon nanotubes was observed to have the same feature. In water-carbon nanotubes interface, a high-density region of water molecules exists around carbon nanotubes. The results reveal that the water orientation around carbon nanotubes is roughly dependent on carbon nanotubes surface charge. The water molecules in close distances to carbon nanotubes were found to make an HOH plane nearly perpendicular to the water-carbon nanotubes interface for carbon nanotubes with negative surface charge. For uncharged carbon nanotubes and carbon nanotubes with positive surface charge, the HOH plane was in tangential orientation with water-carbon nanotubes interface. There was also a significant reduction in hydrogen bond of water region around carbon nanotubes as compared with hydrogen bond in bulk water. This reduction was very obvious for carbon nanotubes with positive surface charge. In addition, the calculation of dynamic properties of water molecules in water-CNT interface revealed that there is a direct relation between the number of Hbonds and self-diffusion coefficient of water molecules.

Key words: Carbon Nanotubes, Water Structure, Hydrogen Bond, Water-Carbon Nanotubes Interface, Molecular Dynamics

INTRODUCTIONS

Carbon nanotubes (CNTs) have a high potential in a large variety of applications due to their special properties, including nanoelectronic devices [2,3], high strength materials [4,5], gas and energy storage systems [6-8], heavy metal ion adsorption process [9-12], and drug delivery [13]. The majority of these applications depend on the wettability of the CNT surface and its hydrophobic-hydrophilic behavior. In addition, the structural properties of fluid and gas around CNT play important roles in the properties of CNTs [14].

The investigations on the structural properties of water molecules surrounding an uncharged CNT show that the water molecules make a shell-like layer around CNT [15]. In addition, some water properties like density and number of hydrogen bonds of water molecules around the CNT surface are subject to change [15,16]. The results also showed that fluids with the surface tension less than 100 mN/m (like water) can wet the CNT surface [17,18].

Most studies on water structure around CNT have been for uncharged CNT, but in the majority of the applications, the CNT surface has positive or negative charge. For example, about CNTs in water the experimental studies proved that the surface charge of CNT is a function of the pH of the solution. There is only a certain pH value named "point of zero charge (PZC)" for which the CNTs are actually uncharged [19-21].

In this investigation, the structural properties of water molecules around CNT were predicted by using molecular dynamics simulation. Various structural properties such as reduced density profile, number of hydrogen bonds per water molecule, and angular distribution functions of HOH plane and OH bonds of water molecules relative to CNT plane have been investigated. We chose five different CNTs having carbon atoms with point charges of –0.01e, –0.05e, 0.0, +0.01e, and 0.05e. The experimental data show that the electrical charges of CNT in different pH vary in the above range [20].

†To whom correspondence should be addressed.
E-mail: ma_mehrabian@alum.mit.edu

SIMULATION DETAILS AND POTENTIAL MODELS

1. Simulation Details

A system consisting of 1557 water molecules, and a (6, 6) CNT was considered in this study. The simulations were carried out using TINKER code Package. The (6, 6) CNT was 12.2 Å in length and 4.13 Å in radius; it was located in the center of a periodic computational box with dimensions of $36.3\times36.3\times12.2$ Å^3. The CNT was considered a rigid body and had a fixed location during the simulation.

The NVT ensemble was applied in the system, and the Berendsen method [22] was used to keep the system at constant temperature of 298 K. The Rattle algorithm was used for integrating the motion equation of molecular dynamic problem with internal constraint. In all simulations, the time step was chosen as small as 0.5fs. This is necessary for simulation of the bonding and bending of the water molecules. The complete simulation required that the MD code runs at 10^5 time step. The first 2×10^4 time steps were necessary to guarantee equilibrium condition between water molecules and CNT. The remaining 8×10^4 time steps were needed to carry out water structural properties.

2. Potential Models

The water molecules in MD can follow different models such as SPC [23], SPC/E [24], and TIP3P [25]. We chose the flexible

TIP3P model for water molecules:

$$U_{Total}=U_{bond}+U_{angle}+U_{vdw}+U_{coulomb} \quad (1)$$

where U_{bond}, and U_{angle} are the bond strength and angle bending energy, respectively. They are defined as

$$U_{bond}=\sum_{bond} k^{bond}(r_{O\text{-}H}-r_{O\text{-}H}^{eq})^2 \quad (2)$$

$$U_{angle}=\sum_{angle} k^{angle}(\theta_{H\text{-}O\text{-}H}-\theta_{H\text{-}O\text{-}H}^{eq})^2 \quad (3)$$

where k_i is the (bond or angle) force constant, $r_{O\text{-}H}$ is the bond length, $r_{O\text{-}H}^{eq}$ is equilibrium bond length, $\theta_{H\text{-}O\text{-}H}$ is the angle between H-O-H, and $\theta_{H\text{-}O\text{-}H}^{eq}$ is the equilibrium angle between H-O-H. The last two terms in Eq. (1) describe the van der Waals (vdW) and electrostatic non-bonded interactions, respectively:

$$U_{vdw}=\sum_i\sum_{j>i}\varepsilon_{ij}\left[\left(\frac{\sigma_{ij}}{r_{ij}}\right)^{12}-2\left(\frac{\sigma_{ij}}{r_{ij}}\right)^{6}\right] \quad (4)$$

$$U_{coulomb}=\sum_i\sum_{j>i}\frac{q_iq_j}{4\pi\varepsilon_0 r_{ij}} \quad (5)$$

We used a simple Lennard-Jones 12-6 potential form to simulate vdW interaction. ε and σ are the well-depth and diameter of the potential [26]. The parameters q_i and q_j are charges of atoms i and j, which are located at the center of the atoms. The van der Waals and electrostatic interactions were used for simulating the interaction between CNT and water molecules and the Lorentz-Berthelot mixing rule can be used for computation of ε and σ between unlike atoms [27]:

$$\varepsilon_{ij}=\sqrt{\varepsilon_i\varepsilon_j},\quad \sigma_{ij}=\frac{(\sigma_i+\sigma_j)}{2} \quad (6)$$

The cutoff distances for vdW and electrostatic forces were considered 9.5 Å. The Lennard-Jones parameters, the bond strength parameters, the angle bending parameters and partial charges used in the present TIP3P water model are listed in Table 1. The Lennard-Jones parameters for CNT potential are listed in Table 2. The simulation was performed for CNT carbon atom charges of 0.05e, 0.01e, 0.0e, −0.001e, and −0.05e.

Table 1. Parameters used in TIP3P model [25]

Symbol	Unit	TIP3P
r_{OH}	[nm]	0.9572
θ_{HOH}	[°]	104.52
ε_{OO}	[kcal/mol]	0.15
σ_{OO}	[nm]	0.315
ε_{HH}	[kcal/mol]	0.0
σ_{HH}	[nm]	0.0
q_O	Electron unit	−0.834
q_H	Electron unit	0.417
k^{bond}	[kcal/(mol·Å^2)]	450.0
k^{angle}	[kcal/mol·rad^2]	55.0

Table 2. Parameters used in CNT potential model [28]

Symbol	Unit	Amount
ε	[kcal/mol]	0.055
σ	[Å]	3.4

RESULTS AND DISCUSSION

1. Water Molecule-CNT Total Energy

The schematic diagram showing the water molecule and CNT

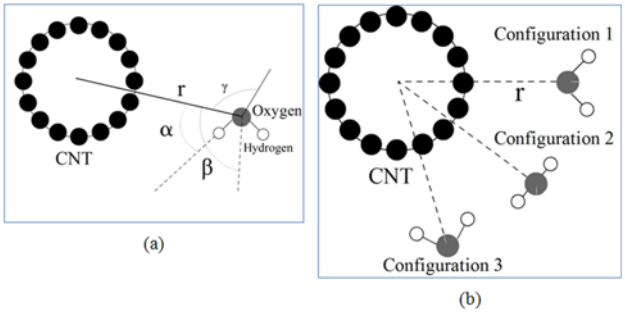

Fig. 1. (a) A schematic diagram of a water molecule and a CNT, α is the angle between OH bond and CNT plane, β is the angle between HOH plane and CNT plane, γ is the angle between the plane of the water molecule and CNT plane. (b) Different configurations: 1- α=127.74, β=180, γ=90; 2- α=90, β=90, γ=180; 3- α=52.26, β=0, γ=90.

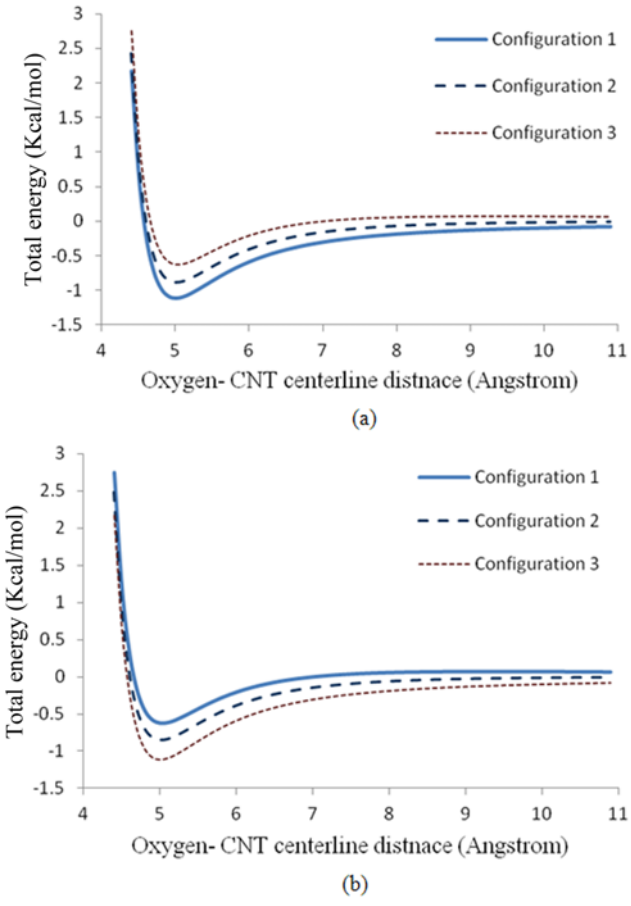

Fig. 2. The total energy between a water molecule and CNT (a) CNT with charge of 0.01e (b) CNT with charge of −0.01e at configurations: 1- α=127.74, β=180, γ=90; 2-α=90, β=90, γ=180; 3- α=52.26, β=0, γ=90.

is in Fig. 1(a). In addition, three special configurations for water molecule and CNT are shown in Fig. 1(b). Fig. 2 demonstrates the total energy between a water molecule and CNT for the above configurations. The total energy is defined as a sum of the vdW energy and the electrostatic energy. As shown in Fig. 2, the total energy is a function of water molecule-CNT distance. In infinite distance, there is no interaction between water molecule and CNT. By decreasing the water molecule-CNT distance, the interaction energy causes attractive energy between water molecule and CNT. In distances shorter than the equilibrium distance, the water molecule and CNT repel each other. The results also show that for CNT with negative and positive surface charges, the first and second stable configurations are 3 and 1, respectively. A more stable configuration is one that has minimum total energy in equilibrium distance. It can be interpreted as the water molecules direction toward CNT is related to CNT charge. For CNT with negative surface charge, the water molecules are in the direction that the hydrogen atoms are located in closer distance to CNT due to attractive electrostatic energy between CNT and hydrogen atoms of water molecule.

2. Water Density Profiles

Fig. 3 demonstrates the water radial density distribution around uncharged CNT. Water radial density profile reveals that there is a high-density region in water-CNT interface located about 3.2 Å away from CNT sidewall. Behind the high water density region, there is also a low-density region that indicates that interaction energy between water molecules and CNT is big enough to create a water layer around CNT. Water density is affected until 6.1-7.2 Å away from CNT sidewall. The results also proved that water molecules around uncharged CNT arranged in the direction that the hydrogen atoms are located in closer distance to CNT. The predictions are in very good agreement with previous studies about water around uncharged (16,0) CNT [15] and graphite sheets [29].

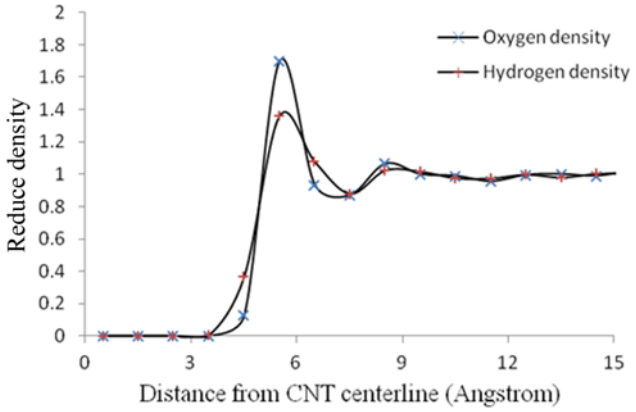

Fig. 3. Water radial density profile for uncharged CNT.

Fig. 4 presents the water radial density profile around CNTs with different surface charges. The water reduced density profile in all

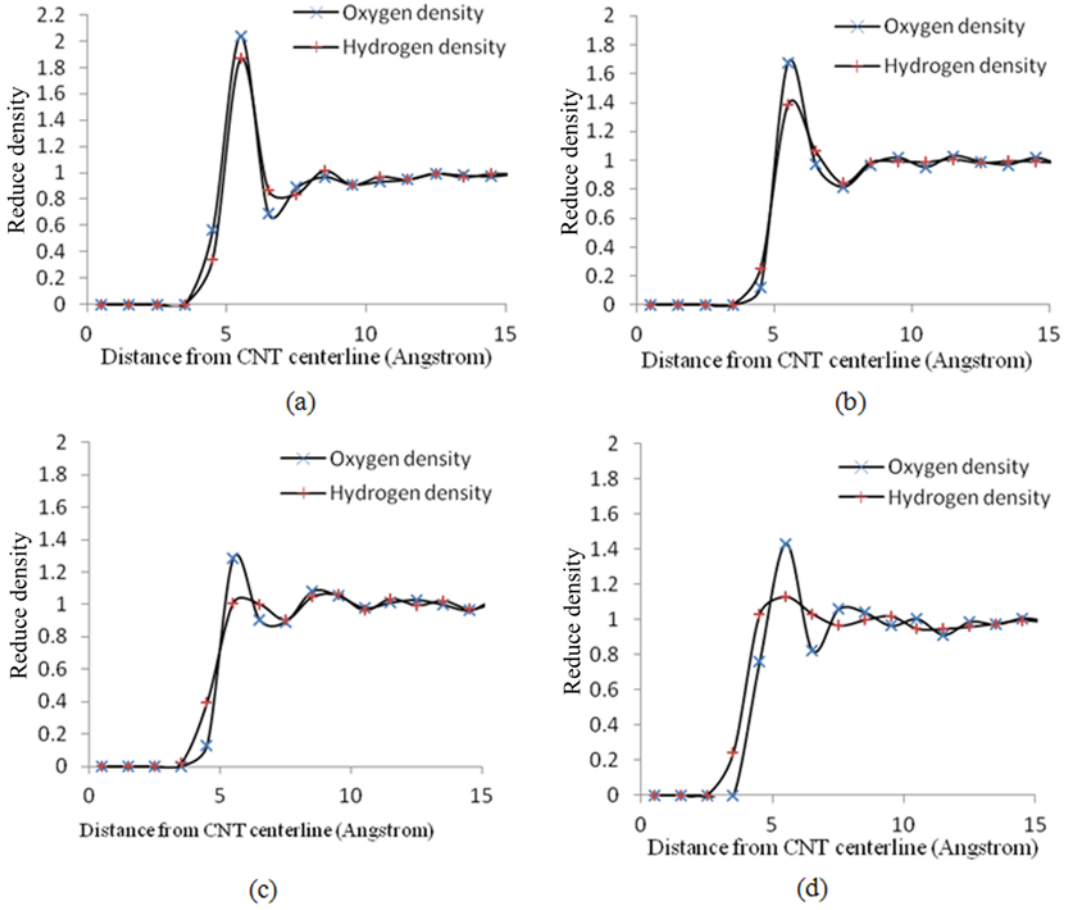

Fig. 4. The water radial density profile for charged CNTs, the carbon atoms of CNT with point charge: (a) +0.05e, (b) +0.01e (c) –0.01e, and (d) –0.05e.

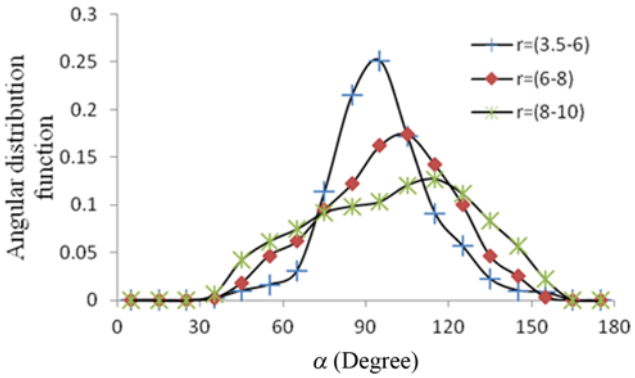

Fig. 5. The ADF of angle α for water molecules around uncharged CNT.

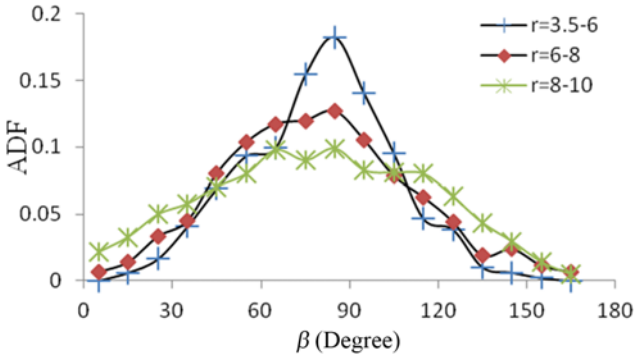

Fig. 7. The ADF of angle β for water molecules around the uncharged CNT.

cases displays a similar pattern like the water density around uncharged CNT [this study, 15] and water around graphite sheets [29]. Nevertheless, the results show some change in density profile due to the electrostatic interaction between water molecules and CNT surface. The results indicated that with increasing the negative surface charge of CNT, the existence of hydrogen atoms is more than oxygen atoms in closer distances from CNT sidewall. These results are in good agreement with the total energy profile corresponding to three configurations shown in Fig. 2, which shows that when CNT has negative surface charge the water molecules are arranged in a direction in which the hydrogen atoms are located in closer distances from CNT. On the other hand, when CNT has maximum positive surface charge (Fig. 4(a)) the oxygen atoms are located a closer distance to CNT because of electrostatic attraction force between CNT and oxygen atoms. With increasing the positive charge of CNT, the water density around the CNT is increased. A similar behavior is observed for increasing the negative charge on CNT surface. However, for net equal positive and negative charges, the value of maximum reduced density for negative charge is lower than that for positive charge.

3. Orientation of Water Molecules

For studying the water molecule orientation relative to CNT, the distribution of the angles α and β are calculated. Fig. 5 shows the OH bond angular distribution function (ADF), angle α, around the uncharged CNT. The ADF is calculated for three ranges of water molecules:

Range 1, 3.5 Å<r<6 Å: first maximum in reduced density profile (water molecules in water-CNT interface).

Range 2, 6 Å<r<8 Å: water molecules contributing the first minimum peak of radial oxygen density profile.

Range 3, 8 Å<r<10 Å: water molecules contributing the second maximum peak of radial oxygen density profile.

The ADF for angle α proves that the OH bonds around the CNT are tangential to the plane of CNT. In contrast, in farther distance from CNT sidewall, the OH bond of water molecules shifts to higher angles to CNT plane. These results are in good agreement with [15].

The ADF of angle α for water molecules around charged CNT are shown in Fig. 6. For every case the angle α is the smaller angle between two OH bonds in a water molecule and CNT plane. The ADF for CNT with negative surface charge indicate the parallel orientations between OH bond and CNT plane. This is due to the attractive force between hydrogen with positive charge and CNT with negative charge. For the CNT with positive surface charge the ADF shows the maximum probability for OH bond angle is about 80°. The positive charge on CNT causes slight distortion and little variation in angle α compared with the negative charge.

To evaluate the orientation of water molecules around CNT, in

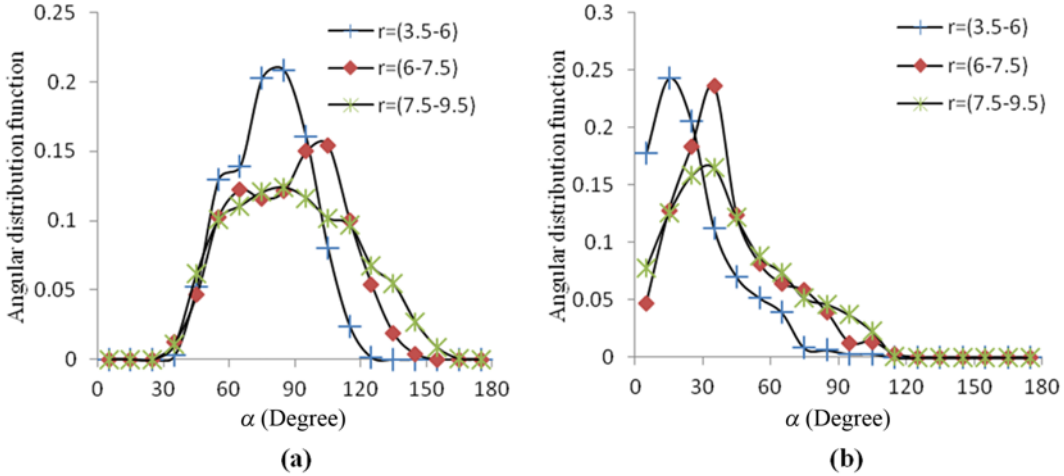

Fig. 6. The ADF of angle α for water molecules around charged CNT's, the carbon atoms of CNT with point charge: (a) +0.05e, (b) –0.05e.

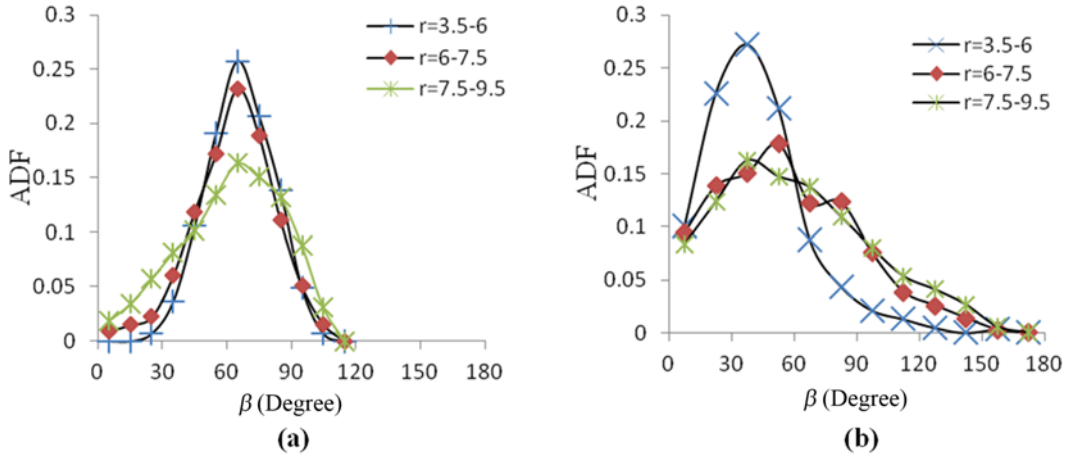

Fig. 8. The ADF of angle β for water molecules around charged CNTs, the carbon atoms of CNT with point charge: (a) +0.05e, (b) –0.05e.

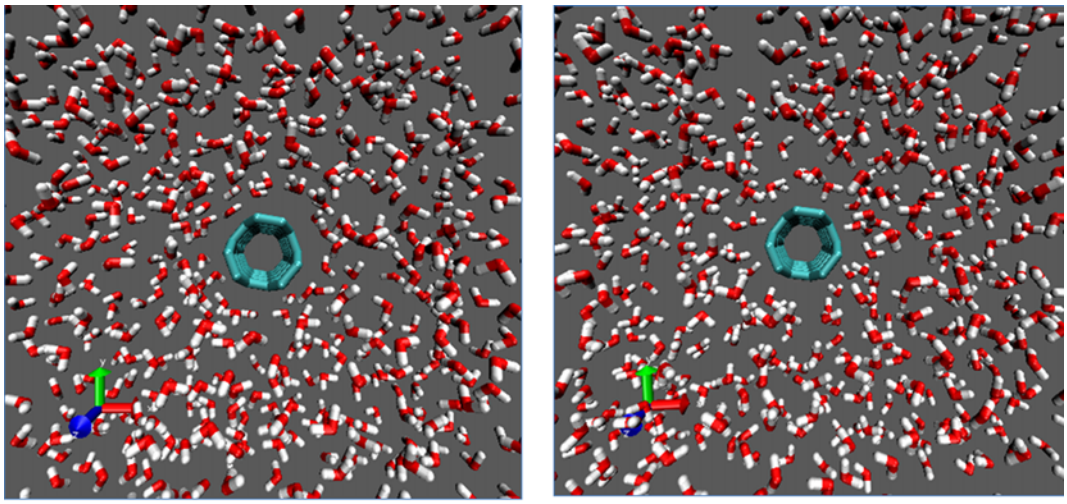

Fig. 9. Snapshot of water molecule around CNT with point charge: (a) +0.05e, (b) –0.05e white denotes hydrogen atoms, red denotes oxygen atoms, and blue denotes CNT atoms.

this investigation the ADF of angle β was also calculated and is shown in Fig. 7 and Fig. 8 for uncharged and charged CNT, respectively. The ADF distribution shows that the water molecules in the vicinity of CNT (Range 1) make an angle of about 90° with CNT plane. For charged CNT, the peak of ADF shifts to lower angles. Fig. 9 demonstrates a snapshot of water molecules around charged CNT. The effect of water orientation due to CNT charge is clearly shown in this figure.

4. Hydrogen Bond

For a better understanding of the water structure around CNT, the mean number of water hydrogen bonds per water molecule (Hbond) is considered. We used a geometrical definition for realizing an Hbond. In this definition, two water molecules are contributing in Hbond when all of three following conditions are satisfied [15,30-31]:

- The distance between both oxygen atoms of two water molecules is smaller than 3.6 Å.
- The distance between the oxygen of acceptor molecule and the hydrogen of the donor is less than 2.4 Å.
- The bond angle between O-O direction and the molecular O-H direction of the donor, where H forms the Hbond, is smaller than 30°.

The number of Hbonds around charged and uncharged CNTs is reported in Table 3. At the nearest distance to CNT, it can be extracted a reduction in number of Hbonds in comparison with bulk water that is 3.7 Hbond per water molecule [31]. This number is

Table 3. The number of Hbonds in different regions around CNT

P. ch.[a]	First maximum in R. D. P[b]	First minimum in R. D. P.	Second maximum in R. D. P[b]
−0.05	3.10	3.4	3.4
−0.01	2.82	3.3	3.4
0.0	2.85	3.4	3.5
+0.01	2.6	3.5	3.5
+0.05	2.23	3.6	3.5

[a]Point charge of CNT carbon atoms
[b]Reduced density profile belong to oxygen density

Table 4. Diffusion coefficients, D, for water molecules in water-CNT interface

P. ch.[a]	D ($\times 10^{-5}$ m^2/s)
−0.05	1.41
−0.01	1.53
0.0	1.62
+0.01	1.02
+0.05	0.96

[a]Point charge of CNT carbon atoms

smaller for CNT with negative charge. For CNT with carbon atom point charge of –0.05e, this reduction is about 0.26%, whereas for CNT with carbon atom point charge of +0.05e, this reduction is more than 0.39%. This is probably due to the effect of CNT on water molecules orientation and water density where at shorter distance than water-CNT interface the number of water molecules goes to zero, and this reduces the opportunity of constraining Hbond. Furthermore, at near distance to CNT, the water molecules orientation is almost the same and this phenomenon causes difficulty in making Hbond between water molecules. The diffusion coefficient of water molecules in water-CNT interface was calculated and reported in Table 4. For calculating D, the mean square displacement (MSD) of water molecules is used which is defined as [27]:

$$D = \frac{1}{6}\lim_{t\to\infty}\frac{MSD}{t} = \frac{1}{6}\lim_{t\to\infty}\frac{\langle[r(t+dt)-r(t)]^2\rangle}{t} \quad (7)$$

Where r is the vector position of water molecule and t is the time. Tables 3 and 4 indicate that a direct relation holds between the number of Hbonds and self-diffusion coefficient. By reducing the dynamic mobility of water molecules in water-CNT interface the number of Hbonds is also decreased. The same behavior is reported in the literature for water molecules around or in the CNTs [32,33] and gold substrate [34].

CONCLUSIONS

A molecular dynamics simulation is used to investigate the structural properties of water molecules around charged and uncharged CNT. The reduced density profile was analyzed and the same pattern observed in density profiles of water molecules around CNTs. A high-density region of water molecules was observed in water-CNT interface. The results reveal the presence of a low-density region behind the high-density region. In the interface region, the hydrogen atoms are located at closer distances to uncharged CNT and CNT with negative surface charge. The maximum reduced density in water-CNT interface belongs to CNT with positive charge. We also found some characteristic properties of water molecules orientation around CNT. In water-CNT interface, the angle between OH bond of water molecule and the plane of uncharged CNT is about 90°. More investigation about water molecules orientation in water-uncharged CNT interface demonstrated a tangential situation of water molecules to CNT plane. At near distance to CNT, an important decrease was also observed in the number of Hbonds relative to bulk water for both charged and uncharged CNT. This distortion of the Hbond network is because of changing of water molecule orientation and water molecule density due to the effect of water-CNT interaction.

NOMENCLATURE

Abbreviations

ADF : angular distribution function
MD : molecular dynamics
P. Ch. : point charge of CNT carbon atoms
R. D. P. : reduced density profile
U_{bond} : bond strength energy [kcal/mol]
U_{angle} : angle bending energy [kcal/mol]
U_{vdW} : van der Waals energy [kcal/mol]
$U_{coulomb}$: electrostatic energy [kcal/mol]

English Symbol

D : diffusion coefficient [m^2/s]
k^{bond} : bond force constant [kcal/(mol·Å^2)]
k^{angle} : bond force constant [kcal/mol]
q : atom point charge, e
r : distance [Å]
$r_{O\text{-}H}$: bond length [Å]
$r^{eq}_{O\text{-}H}$: equilibrium bond length [Å]
U_{total} : total potential energy [kcal/mol]
t : time [s]

Greek Symbols

Å : angstrom [10^{-10} m]
$\theta_{H\text{-}O\text{-}H}$: angle between H-O-H [degree]
$\theta^{eq}_{HO\text{-}H}$: equilibrium angle between H-O-H [degree]
ε : well-depth of potential [kcal/mol]
ε_0 : permittivity of free space [8.8542×10^{-12} $C^2N^{-1}m^{-2}$]
σ : diameter of the potential [Å]

Units

Å : angstrom [10^{-10} m]
e : electron unit [1.6×10^{-19} C]

REFERENCES

1. S. Iijima and T. Ichihashi, *Nature*, **363**, 603 (1993).
2. A. Javey, J. Guo, D. B. Farmer, A. Wang, D. Wang, R. G. Gordon, A. Lundstrom and H. Dai, *Nano Lett.*, **4**, 447 (2004).
3. L. Dong, X. Tao, L. Zhang, X. Zhang and B. J. Nelson, *Nano Lett.*, **7**, 58 (2007).
4. L. G. Zhou and S. Q. Shi, *Comput. Mater. Sci.*, **23**, 166 (2002).
5. Z. Yao, Ch. Zhu, M. Cheng and J. Liu, *Comput. Mater. Sci.*, **22**, 180 (2001).
6. Ch. Gu, G. H. Gao, Y. X. Yu and Z. Q. Mao, *Int. J. Hydrog. Energy*, **26**, 691 (2001).
7. P. A. Gordon and R. B. Saeger, *Ind. Eng. Chem. Res.*, **38**, 4647 (1999).
8. S. Y. Li, X. H. Zeng, N. Q. Jin, H. Y. Zhang and X. Zhang, *Phys. Lett. A*, **372**, 1303 (2008).
9. G. Rao, Ch. Lu and F. Su, *Separation and Purification Technology*, **58**, 224 (2007).
10. H. J. Wang, A. L. Zhou, F. Peng, H. Yu and L. F. Chen, *Mater. Sci.*

Eng. A, **466**, 201 (2007).
11. Y. H. Li, S. Wang, J. Wei, X. Zhang, C. Xu, Z. Luan, D. Wu and B. Wei, *Chem. Phys. Lett.*, **357**, 263 (2002).
12. M. Bahgat, A. A. Farghali, W. M. A. El Rouby and M. H. Khedr, *J. Anal. Appl. Pyrol.*, **92**(2), 307 (2011).
13. F. Martin, R. Walczak, A. Boiarski, M. Cohen, T. West, C. Cosentino and M. Ferrari, *J. Controlled Release*, **102**, 123 (2005).
14. S. Shokri, R. Mohammadikhah, H. Abolghasemi, A. Mohebbi, H. Hashemipour, M. Ahmadi-Marvast and Sh. JafariNejad, *Int. J. Chem. Eng. Appl.*, **1**, 63 (2010).
15. J. H. Walther, R. Jaffe, T. Halicioglu and P. Koumoutsakos, *J. Phys. Chem. B*, **105**, 9980 (2001).
16. J. H. Walther, R. Jaffe, E. M. Kotsalis, T. Werder, T. Halicioglu and P. Koumoutsakos, *Carbon*, **42**, 1185 (2004).
17. E. Dujardin, T. W. Ebbesen, H. Hiura and K. Tanigaki, *Science*, **265**, 1850 (1994).
18. E. Dujardin, T. W. Ebbesen, A. Krishnan and M. M. J. Treacy, *J. Adv. Mater.*, **10**(17), 1472 (1998).
19. A. Stafiej and K. Pyrzynska, *Microchem. J.*, **89**, 29 (2008).
20. C. Lu and H. Chiu, *Chem. Eng. Sci.*, **61**, 1138 (2006).
21. H. P. Boehm, *Carbon*, **40**, 145 (2002).
22. H. J. C. Berendsen, J. P. M. Postma, W. F. van Gunsteren, A. DiNola and J. R. Haak, *J. Chem. Phys.*, **81**, 3684 (1984).
23. H. J. C. Berendsen, J. P. M. Postma, W. F. van Gunsteren and J. Hermans, *Reidel Dordrecht*, 331 (1981).
24. H. J. C. Berendsen, J. R. Grigera and T. P. Straatsma, *J. Phys. Chem.*, **91**, 6269 (1987).
25. P. Mark and L. Nilsson, *J. Phys. Chem. A*., **105**, 9954 (2001).
26. P. DAngelo, V. Migliorati, G. Mancini and G. Chillemi, *J. Phys. Chem. A*, **112**, 11833 (2008).
27. M. P. Allen and D. J. Tildesley, *Computer simulation of liquids*, Clarendon Press, Oxford, Hardback (1987).
28. S. Banerjee, A. Murad and I. K. Puri, *Chem. Phys. Lett.*, **434**, 292 (2007).
29. D. E. Ulberg and K. E. Gubbins, *Mol. Phys.*, **84**(6), 1139 (1995).
30. J. Marti, *J. Chem. Phys.*, **110**, 6876 (1999).
31. M. C. Gordillo and J. Marti, *Chem. Phys. Lett.*, **341**, 250 (2001).
32. J. A. Thomas and A. J. H. McGaughey, *J. Chem. Phys.*, **128**, 084715 (2008).
33. Q. Z. Yuan and Y. P. Zhao, *J. American Chem. Soc.*, **131**, 6374 (2009).
34. Y. Quanzi and Y. Zhao, *Phys. Rev. Lett.*, **104**, 246101 (2010).